A proteasomal ATPase contributes to dislocation of endoplasmic reticulum-associated degradation (ERAD) substrates

Carni Lipson, Guy Alalouf, Monika Bajorek, Efrat Rabinovich, Avigail Atir-Lande, Michael Glickman, Shoshana Bar-Nun

THE JOURNAL OF BIOLOGICAL CHEMISTRY VOL. 283, NO. 11, pp. 7166–7175, March 14, 2008

A Proteasomal ATPase Contributes to Dislocation of Endoplasmic Reticulum-associated Degradation (ERAD) Substrates*

Received for publication, July 18, 2007, and in revised form, January 3, 2008 Published, JBC Papers in Press, January 3, 2008, DOI 10.1074/jbc.M705893200

Carni Lipson[‡1], Guy Alalouf[‡1], Monika Bajorek[§2], Efrat Rabinovich[‡], Avigail Atir-Lande[§], Michael Glickman[§], and Shoshana Bar-Nun[‡3]

From the [‡]Department of Biochemistry, George S. Wise Faculty of Life Sciences, Tel Aviv University, Tel Aviv 69978, Israel and the [§]Department of Biology, Technion-Israel Institute of Technology, Haifa 32000, Israel

Endoplasmic reticulum (ER)-associated degradation (ERAD) eliminates aberrant proteins from the ER by dislocating them to the cytoplasm where they are tagged by ubiquitin and degraded by the proteasome. Six distinct AAA-ATPases (Rpt1–6) at the base of the 19S regulatory particle of the 26S proteasome recognize, unfold, and translocate substrates into the 20S catalytic chamber. Here we show unique contributions of individual Rpts to ERAD by employing equivalent conservative substitutions of the invariant lysine in the ATP-binding motif of each Rpt subunit. ERAD of two substrates, luminal CPY*-HA and membrane 6myc-Hmg2, is inhibited only in *rpt4R* and *rpt2RF* mutants. Conversely, *in vivo* degradation of a cytosolic substrate, ΔssCPY*-GFP, as well as *in vitro* cleavage of Suc-LLVY-AMC are hardly affected in *rpt4R* mutant yet are inhibited in *rpt2RF* mutant. Together, we find that equivalent mutations in *RPT4* and *RPT2* result in different phenotypes. The Rpt4 mutation is manifested in ERAD defects, whereas the Rpt2 mutation is manifested downstream, in global proteasomal activity. Accordingly, *rpt4R* strain is particularly sensitive to ER stress and exhibits an activated unfolded protein response, whereas *rpt2RF* strain is sensitive to general stress. Further characterization of Rpt4 involvement in ERAD reveals that it participates in CPY*-HA dislocation, a function previously attributed to p97/Cdc48, another AAA-ATPase essential for ERAD of CPY*-HA but dispensable for proteasomal degradation of ΔssCPY*-GFP. Pointing to Cdc48 and Rpt4 overlapping functions, excess Cdc48 partially restores impaired ERAD in *rpt4R*, but not in *rpt2RF*. We discuss models for Cdc48 and Rpt4 cooperation in ERAD.

Misfolded proteins and orphan subunits of oligomeric proteins may account for up to 30% of newly synthesized proteins (1). Such aberrant proteins are deleterious to the cell and therefore must be eliminated (2). In the endoplasmic reticulum (ER),[4] quality control mechanisms assure that aberrant proteins are not exported; instead, they are usually dislocated to the cytosol and degraded by the ubiquitin-proteasome system in a process termed ER-associated protein degradation (ERAD; for reviews see Refs. 3–5). Once selected for ERAD, both membrane and luminal proteins are dislocated from the ER back to the cytosol, tagged by polyubiquitin, and delivered for their irreversible proteolysis by the 26S proteasome (6).

The cytosolic p97/Cdc48 ATPase complex appears to provide the driving force for the dislocation of ERAD substrates. This homo-hexameric AAA-ATPase along with its cofactors Ufd1 and Npl4 was shown to be essential for ERAD (7–12). Involvement of the p97/Cdc48 complex in the dislocation step was demonstrated by the inhibiting effect of p97 dominant negative variant on dislocation of MHC class I heavy chain in semi-intact mammalian cells (8) and by the hampered release of CPY* to the cytosol in the *ufd1-1* mutant (10). In the *cdc48-10* mutant, CPY* remained trapped within the ER lumen as non-ubiquitinated protein, pointing to Cdc48 as the driving force for passage across ER membranes (12). The ability of p97/Cdc48 to pull ERAD substrates out of the ER is probably a consequence of conformational changes of p97 during its ATPase cycle, which translate ATP hydrolysis into mechanical forces (13), and the underlying activity of AAA-ATPases in unfolding and disassembling proteins (14).

An alternative candidate to provide the driving force for dislocation of ERAD substrates is the proteasome. Being a limiting factor in the entire ubiquitin-dependent proteolytic pathway, proteasomes greatly influence system capacity and the substrates degradation rate, including ERAD (15, 16). Yet, in addition to its established function in proteolysis at the end step of the pathway, the 26S proteasome may also participate in earlier steps, such as dislocation of ERAD substrates. Mechanistically, proteasome association with ER membranes would facilitate its function in pulling substrates out of the ER. Indeed, a proteasome subpopulation is associated with the ER (for reviews see Refs. 17, 18). The two subcomplexes of the 26S proteasome, the 20S catalytic particle (CP) and the ATPase-containing 19S regulatory particle (RP), were implicated in dislocation. The pro-

* This work was supported in part by grants from Israel Science Foundation (ISF) and United States-Israel Binational Science Foundation (BSF) (to S. B. N.) and grants from ISF and BSF (to M. H. G.). The costs of publication of this article were defrayed in part by the payment of page charges. This article must therefore be hereby marked "*advertisement*" in accordance with 18 U.S.C. Section 1734 solely to indicate this fact.

[1] These authors contributed equally to this work.
[2] Present address: Dept. of Biochemistry, University of Utah, 20 North 1900 East SLC, UT 84132-3201.
[3] To whom correspondence should be addressed. Tel.: 972-3-6408984; Fax: 972-3-6406834; E-mail: shoshbn@tauex.tau.ac.il.

[4] The abbreviations used are: ER, endoplasmic reticulum; CP, catalytic particle; ERAD, ER-associated protein degradation; RP, regulatory particle; UPR, unfolded protein response; HA, hemagglutinin; GFP, green fluorescent protein; X-gal, 5-bromo-4-chloro-3-indolyl-β-D-galactoside.

teolytic activity of β-subunits within the 20S CP was shown to be required for the extraction of several ERAD substrates from the ER (10, 19). Nevertheless, the proteolytic activity of the proteasome does not constitute a general pulling mechanism, as exemplified by ERAD of luminal μs, the heavy chain of secretory IgM, in B lymphocytes (12, 20). Although μs interacted exclusively with ER-bound proteasomes, blockers of proteasomal proteolytic activity had no effect on passage of μs across ER membranes, yet they inhibited subsequent μs release from the ER cytosolic face (12).

The 19S RP was also implicated in dislocation and was proposed as the sole driving force for dislocation of pro-alpha factor *in vitro* (21). The 19S RP is composed of a base subassembly that contains six AAA-ATPase subunits (Rpt1–6) alongside three non-ATPase subunits (Rpn1, Rpn2, Rpn10) and a lid subparticle that encompasses eight stoichiometric subunits (Rpn3, Rpn5, Rpn6, Rpn7, Rpn8, Rpn9, Rpn11, and Rpn12) (22–24). The chaperone-like activity of the Rpt AAA-ATPases (25) is crucial for their ability to unfold protein substrates and translocate them through the gated channel into the 20S CP proteolytic chamber. Binding of the 19S RP to the surface of the 20S CP opens the narrow entrance gated by the N-terminal tails of the α-subunits and allows access of protein substrates into the proteolytic chamber for proteolysis (26–28). In addition, the Rpt subunits may be involved in binding or anchoring polyubiquitinated substrates since at least one of them, Rpt5/S6, interacts with polyubiquitin chains (29). Whether each Rpt AAA-ATPase contributes to ERAD differentially is not clear, and the possibility that distinct sets of Rpt subunits participate preferentially in ERAD or cytosolic/nuclear degradation has been partially explored. Studies with yeast mutants such as *cim5-1*(*rpt1*), *rpt1S*, *rpt2RF*, *rpt4R*, *rpt5S* and *cim3-1*(*rpt6*) demonstrated involvement of Rpt subunits in ERAD (6, 10, 19, 30). Subunit Cim5/Rpt1 was involved in extracting membrane ERAD substrates (19), and subunits Rpt4 and Rpt5, but not Rpt2, were also implicated in ERAD (10). The luminal ERAD substrate CPY* was stabilized in the ATPase mutants *rpt4R* and *rpt5S* but hardly in *rpt2RF* (10). However, a small but significant proportion of CPY* remained protease-sensitive in *rpt4R*, suggesting that protein dislocation could occur independently of Rpt4 ATPase (10). Hence, it was concluded that p97/Cdc48/Ufd1/Npl4 complex rather than the Rpt subunits provided the driving force for extracting ERAD substrates from the ER (10).

Intrigued by the possibility that distinct sets of proteasomal AAA-ATPases might be engaged in unique processes along the ERAD pathway, we systematically studied individual contributions of the ATPase activity of each of the six 19S AAA-ATPases to proteasomal degradation globally and to ERAD and dislocation of ERAD substrates in particular. To that end, we utilized a set of six mutant strains in which each *RPT* gene was replaced by an equivalent mutant version with conservative substitutions of the invariant lysine of the Walker A ATP-binding motif (31). This substitution generally results in complete or partial inhibition of ATP binding and ATP hydrolysis (32). This set of strains allows us to elucidate roles of individual Rpt subunits in the various ERAD steps and to study their interrelation with another AAA-ATPase implicated in ERAD, p97/Cdc48, in fulfilling their multiple functions in ERAD. We found that out of the six equivalent mutated Rpt subunits, only *rpt2RF* and *rpt4R* displayed impaired ERAD. However, while the Rpt2 mutation disrupted general proteasomal degradation, the Rpt4 mutation was manifested in impaired dislocation of ERAD substrates, an outcome that was partially restored by excess Cdc48.[5]

EXPERIMENTAL PROCEDURES

Yeast Strains, Media, and Plasmids—Strain SUB62 (*MAT*a *his3*-D*200 lys2-801 leu2-3,112 trp1-1 ura3-52*) is the isogenic wild-type of the equivalent *rpt* mutant strains *rpt1S* DY106, *rpt2RF* DY62, *rpt3R* DY93, *rpt4R* DY219, *rpt5R* DY155, and *rpt6R* DY100, individually mutated in their invariant ATP-binding lysine (31). Defective ERAD was previously shown in *cdc48-10* at 37 °C (9). The *pre1-1* strain harbors a proteasomal β-subunit defective in chymotrypsin-like activity at 37 °C (33). CPY*-HA (*prc1-1* allele; plasmid pBG15) and 6myc-Hmg2 (plasmid pRH244) were previously described (9, 12). ΔssCPY*-GFP was expressed from plasmid POW0668 ((34); generously provided by D. Wolf, Stuttgart University). To replace *LEU2* with *TRP1* selection marker in Cdc48 expressing plasmid, the *CDC48* gene was excised from pKF700 plasmid (generously provided by K. U. Fröhlich, Graz University) by HindIII, blunt-ended and inserted into a SmaI site in the 2-μm ori-type pAMT20 shuttle vector.

Growth Sensitivity to Tunicamycin, Cadmium, Canavanine, and Temperature—Yeast strains grown to equal cell density were spotted on plates as 10-fold serial dilutions. Deficiencies in the ubiquitin-proteasome pathway were monitored either as a temperature-sensitive phenotype or on arginine-deficient plates supplemented with the arginine analog, canavanine (3 μg/ml) (31, 35). Deficiencies in ERAD were monitored on plates supplemented with $CdCl_2$ (30 μM) (36, 37) or with tunicamycin (2 μg/ml) (38).

Unfolded Protein Response (UPR) Activation—UPR activation was measured with the UPRE-lacZ reporter construct (39). Activity of β-galactosidase was detected on 5-bromo-4-chloro-3-indolyl-β-D-galactoside (X-gal) reporter plates. The maximal induction of UPR was achieved with tunicamycin (2 μg/ml) (40).

Proteasomal Degradation of CPY-HA, 6myc-Hmg2, and ΔssCPY*-GFP, Cell Fractionation and Protease Protection Assay*—Degradation at 30 or 37 °C was followed by immunoblotting of cells collected at indicated time points after addition of cycloheximide (150 μg/ml), lysed and resolved by SDS-PAGE (9). Dislocation of CPY*-HA was monitored by cell fractionation and protease protection assay, as previously described (12). Briefly, postnuclear supernatant (1,000 × *g*, 10 min) from disrupted spheroplasts was treated with trypsin (0.5 mg/ml, 30 min, 4 °C) with or without Triton X-100 (1% v/v), and microsomal pellets and cytosolic supernatants were separated by centrifugation (10,000 × *g*, 30 min, 4 °C). CPY*-HA immunoprecipitated with an anti-HA antibody was resolved by SDS-PAGE and immunoblotted.

[5] Some preliminary results relating to this article were presented in a Symposium on Ubiquitin in Biology and Medicine, in honor of Nobel Laureates Avram Hersko and Aaron Ciechanover, Israel Academy of Sciences and Humanities, October 31, 2005. This lecture was published in Ref. 60.

Immunoprecipitation and Immunoblotting—Immunoprecipitation of detergent-dissolved samples and immunoblotting of immunoprecipitated proteins or total cellular proteins were previously described (9, 12). Primary antibodies: mouse anti-HA (clone 12CA5); mouse anti-Myc (clone 9E10); rabbit anti-Cdc48 (generously provided by K. U. Fröhlich); mouse anti-CPY (clone 10A5-B5; New Biotechnology); chicken anti-Rpt1; rabbit anti-Rpt5 (Affinity Biomol); rabbit anti-Sec61 (generously provided by N. Nelson). Horseradish peroxidase-conjugated secondary antibodies: goat anti-mouse IgG (Jackson), goat-anti-rabbit IgG (Sigma); rabbit anti-chicken (Chemicon). The horseradish peroxidase was visualized by enhanced chemiluminescence (ECL) reaction.

Proteasome In-gel Peptidase Activity Assay—Non-denaturing PAGE of intact 26S proteasomes directly resolved from whole cell extracts, gels incubation with the fluorogenic peptide Suc-LLVY-AMC as a peptidase substrate, and the in-gel visualization of proteasome assembly species by UV light were previously described (15, 31, 41). To estimate the total amount of all proteasome species, regardless of their relative activities, salt-induced dissociation of 20S CP and 19S RP was carried out prior to subjecting samples to non-denaturing PAGE, followed by 20S CP activation in gels incubated for 10 min in buffer with Suc-LLVY-AMC substrate and supplemented with 0.02% (w/v) SDS as described previously (15, 31, 41).

RESULTS

Proteasomal Rpt Subunits Are Not Identical and Indeed Equivalent Mutations Are Distinctively Manifested in Turnover of Luminal and Membrane ERAD Substrates—The obligatory ATP-requiring steps in proteasomal degradation are assumed to include substrate unfolding by the 19S and translocation into the 20S (25, 26, 28, 42, 43). However, the six Rpt AAA-ATPases at the base of the 19S are functionally non-equivalent, as shown by a comparative study of equivalent conservative mutations in the invariant lysine in the Walker A motif of each of the six *RPT* genes. These strains exhibit diverse phenotypes vis-à-vis growth sensitivity to temperature and amino acid analogs, protein degradation *in vivo* and proteolytic activities of purified proteasomes *in vitro* (31). To assess whether their non-equivalence could be extended to ERAD, possibly uncovering unique roles for proteasomal ATPases in this pathway, we tested the degradation of ERAD substrates in wild-type, in *rpt2RF*, *rpt3R, rpt4R, rpt5R, rpt6R* (harboring a conservative lysine-to-arginine substitution) and in *rpt1S* (harboring a non-conservative substitution) (31).

Using the above mutants, we assessed the contribution of each Rpt subunit to ERAD of two well-established topologically distinct ERAD substrates. Luminal CPY*-HA is an HA-tagged version of the unstable point mutant (G255R) of the soluble vacuolar protein carboxypeptidase Y (6), while membrane 6myc-Hmg2 is an unstable Myc-tagged version of the 3-hydroxy-3-methylglutaryl-CoA reductase (44). As shown in Fig. 1, we estimated the half-life of CPY*-HA in each *rpt* mutant by employing the cycloheximide chase assay. In the wild-type (SUB62), $t_{½}$ was under 1 h. Similar degradation rates were measured in *rpt1*, *rpt3*, and *rpt5* mutants ($t_{½} \sim 55$ min), and only a slightly reduced turnover rate was observed in *rpt6*

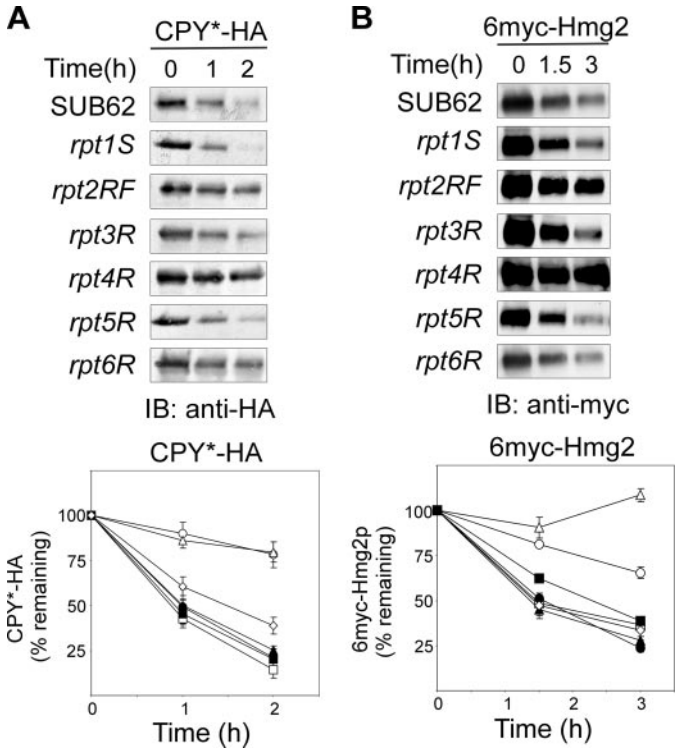

FIGURE 1. **Turnover of luminal and membrane ERAD substrates in *rpt* mutants.** Degradation of CPY*-HA (*A*) and 6myc-Hmg2 (*B*) was followed in wild-type (SUB62), and the indicated *rpt* ATPase mutants. Cycloheximide (150 μg/ml) was added, equal amounts of cells (2 A_{600}) were collected at the indicated time points, lysed, total cellular proteins were resolved by SDS-PAGE, and immunoblotted (*IB*) with the respective anti-HA or anti-Myc antibodies. Graphs illustrate degradation as amounts of remaining substrates as % of their levels upon cycloheximide addition (100%), estimated by densitometry and calculated as average (±S.E.) of five independent experiments represented by the presented blots. Half-life values were calculated from slopes of exponential curves (see text). Wild-type (SUB62), *open squares*; *rpt1S*, *closed squares*; *rpt2RF*, *open circles*; *rpt3R*, *closed circles*; *rpt4R*, *open triangles*; *rpt5R, closed triangles*; *rpt6R*, *open diamonds*.

mutant ($t_{½} \sim 80$ min). However, degradation of CPY*-HA was markedly impaired in *rpt2RF* and *rpt4R* strains with extended $t_{½}$ values approaching 6 h (Fig. 1*A*). This result clearly points to non-equivalence of Rpt subunits also in ERAD.

We next determined whether the impaired degradation of CPY*-HA in *rpt2RF* and *rpt4R* reflected a general ERAD phenomenon, or was specific to this substrate. For this purpose, we followed ERAD of membrane 6myc-Hmg2. Once again, 6myc-Hmg2 was rapidly degraded in wild-type ($t_{½} \sim 1.8$ h), yet markedly stabilized in *rpt2RF* and to an even greater extent in *rpt4R*, with extended $t_{½}$ values approaching 5 h and 20 h, respectively (Fig. 1*B*). The other *rpt* mutations affected 6myc-Hmg2 degradation only slightly, with $t_{½}$ values ranging from 1.5 to 2.2 h (Fig. 1*B*). Hence the degradation patterns of membrane 6myc-Hmg2 or luminal CPY*-HA resemble each other, indicating that only Rpt2 and Rpt4 mutants are manifested in impaired ERAD.

Turnover of a Cytosolic Substrate Distinguishes Rpt2, a Participant of General Proteasomal Degradation, from Rpt4, Which Contributes Preferentially to ERAD—The stabilization of ERAD substrates in *rpt2RF* concurs with the central role of Rpt2 in mediating channel opening into the gated proteolytic chamber (28) and as such in promoting degradation of multiple substrates tested so far (31, 45–47). The stabilization of ERAD

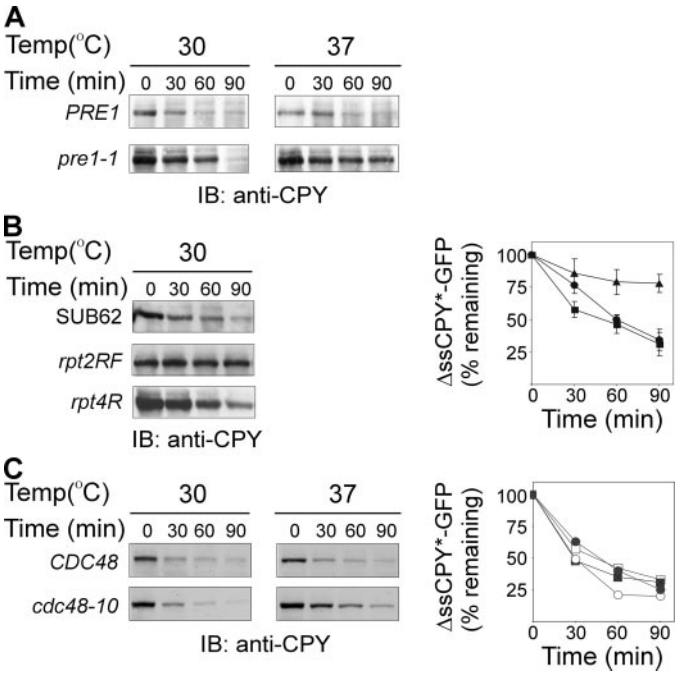

FIGURE 2. **Turnover of a cytosolic substrate in *rpt* and *cdc48* mutants.** Degradation of cytosolic ΔssCPY*-GFP was measured in *pre1-1* (*A*), *rpt2RF* and *rpt4R* (*B*), and *cdc48–10* (*C*), compared with their corresponding wild-type strains: *PRE1* (*A*), SUB62 (*B*), and *CDC48* (*C*). Following 2 h of preincubation at the indicated temperatures, cycloheximide (150 μg/ml) was added, equal amounts of cells (3 A_{600}) were collected at the indicated time points, lysed, total cellular proteins were resolved by SDS-PAGE and immunoblotted (*IB*) with an anti-CPY antibody. Graphs illustrate degradation of ΔssCPY*-GFP as amounts of remaining substrate estimated by densitometry and calculated as % of its level upon cycloheximide addition (100%). The data points in graph *B* are the average (±S.E.) of six independent experiments represented by blot *B*. *Graph C* was calculated from blot *C*. Half-life values (see text) were calculated from slopes of exponential curves. *B*, SUB62, *squares*; *rpt2RF*, *triangles*; *rpt4R*, *circles*; *C*, *CDC48*, *squares*; *cdc48-10*, *circles*; 30 °C, *open symbols*; 37 °C, *closed symbols*.

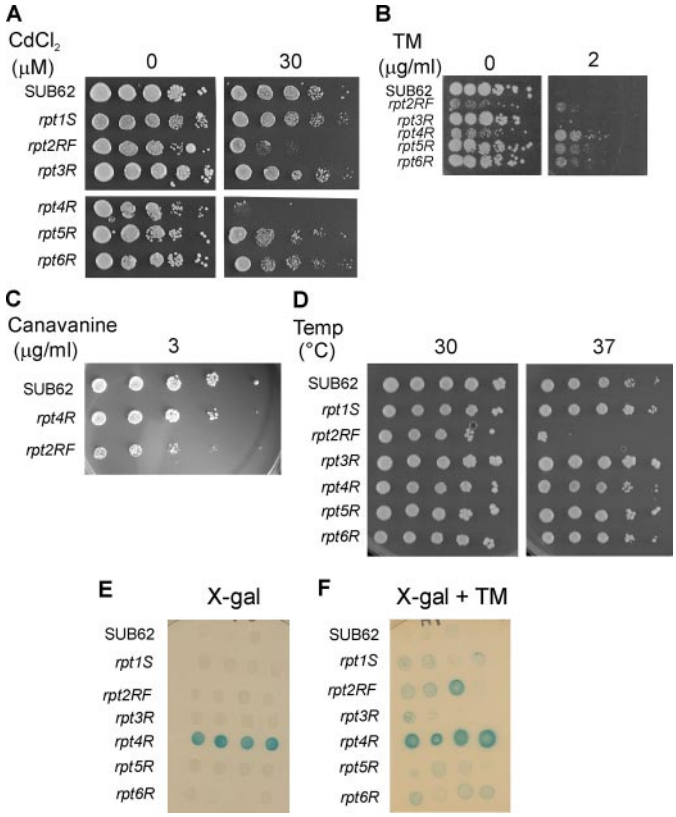

FIGURE 3. **The various *rpt* mutants display distinct sensitivity to general and ER stress conditions and exhibit differential UPR activation.** In the indicated *rpt* mutants or their SUB62 wild-type strain, growth of 10-fold serial dilutions was monitored on plates supplemented with the indicated concentrations of $CdCl_2$ (*A*) or tunicamycin (*B*), on arginine-deficient plates supplemented with canavanine (*C*) or at elevated temperatures (*D*). UPR activation was measured in 4 individual clones as β-galactosidase activity detected on X-gal reporter plates (*E*) and for maximal induction, the X-gal plates were supplemented with tunicamycin (2 μg/ml) (*F*)

substrates in *rpt4R* may also reflect a general role in proteasomal degradation. Alternatively, Rpt4 may contribute preferentially to ERAD, as implied by the pronounced stabilization of both ERAD substrates we tested.

To differentiate between these options, degradation of a cytosolic substrate of the proteasome was monitored. As the closest relative of the luminal ERAD substrate CPY*-HA, we selected ΔssCPY*-GFP (34), as both substrates encompass an identical CPY* domain (the HA and GFP tags exerted no effect on degradation). Lacking a signal sequence, ΔssCPY*-GFP remained in the cytosol and, as expected, it was stabilized in the proteasomal β-subunit temperature sensitive mutant *pre1-1* at 37 °C (Fig. 2*A*), confirming its proteasomal degradation. Clearly, in the *rpt2RF* mutant ΔssCPY*-GFP was stabilized and the 30–50-min half-life of this cytosolic substrate was extended to values approaching 4 h (Fig. 2*B*). Interestingly, degradation of cytosolic ΔssCPY*-GFP proceeded unabated in *cdc48-10* at 37 °C (Fig. 2*C*), contrary to the dramatic stabilization of CPY*-HA (12). This different behavior reflects the role of Cdc48 in dislocation of ERAD substrates, a step that is bypassed by the cytosolic ΔssCPY*-GFP. More importantly, ΔssCPY*-GFP turnover was not affected in *rpt4R* and its $t_{½}$ remained shorter than 1 h, as in the wild-type strain (Fig. 2*B*). This was in a stark contrast to the 6-fold stabilizing effects of *rpt4R* on the degradation of the ERAD substrate CPY*-HA (Fig. 1*A*) and of the *rpt2RF* mutant on the degradation of ΔssCPY*-GFP (Fig. 2*B*). We conclude that the primary outcome of the mutation in Rpt4 studied here is defects in ERAD, suggesting that Rpt4 plays a unique role in this pathway. This is an exciting example of a discriminatory role of an ATPase that is part of a complex of multiple ATPases.

Sensitivity to Stress Conditions and UPR Induction Supports Preferential Involvement of Rpt4 in ERAD Compared with General Proteasomal Functions for Rpt2—Reflecting the relative importance of the Rpt subunits in preparing substrates for proteolysis, *rpt* mutants are sensitive to elevated temperature or amino acid analogs (31). To assess their participation in ERAD, we compared the sensitivity of these *rpt* mutants to ER stress by growing them on plates supplemented with either cadmium (Fig. 3*A*) or tunicamycin (Fig. 3*B*). Although mechanism(s) underlying its toxicity are not fully understood, cadmium generates stress by reacting with thiol groups prevalent in the ER and replacing zinc and iron in metalloproteins, and therefore may reflect ERAD deficiencies (36, 37, 48). Conversely, tunicamycin is known to elicit ER stress by inhibiting *N*-glycosylation of newly synthesized glycoproteins (38), a process that occurs only within the ER lumen. The sensitivity of *rpt* mutants to cadmium (Fig. 3*A*) or tunicamycin (Fig. 3*B*) was compared with

their ability to grow at elevated temperatures (Fig. 3*C*) or in the presence of the arginine analog, canavanine (Fig. 3*D*), conditions that lead to general stress. Clearly, *rpt2RF* was most sensitive to elevated temperature and canavanine (Fig. 3, *C* and *D*) reflecting the general role of Rpt2 in the ubiquitin-proteasome system. The hypersensitivity of *rpt4R* to cadmium (Fig. 3*A*) suggested that Rpt4 was preferentially involved in ERAD. This notion was corroborated by the growth of *rpt4R* on tunicamycin (Fig. 3*B*). Although *rpt2RF* and *rpt4R* were slow growing mutants, *rpt4R* was fully resistant and grew even better in the presence of tunicamycin, under conditions that this drug was toxic to the wild-type strain and to every other *rpt* mutant (Fig. 3*B*). This unexpected result could be explained by our finding that *rpt4R* cells exhibited constitutively activated UPR (Fig. 3*E*) and remarkable induction of this response when treated with tunicamycin (Fig. 3*F*), a known UPR inducer (40) that also revealed the expression of UPRE-lacZ in the wild-type and all the *rpt* mutant strains. These results demonstrated that *rpt4R* mutant accumulated unfolded proteins in the ER, suggesting a preferential role for Rpt4 in ERAD and in particular, in dislocation of ERAD substrates.

Rpt4R-containing Proteasomes Are Structurally Stable, Proteolytically Active, and Capable for ER Association—To explore whether the ERAD defects that we uncovered in *rpt4R* resulted from altered structure or function of the proteasome, we assessed the assembly states and proteolytic activity of proteasomes obtained from wild-type, *rpt2RF*, and *rpt4R* strains. Total cell lysates were resolved by non-denaturing gel electrophoresis and proteasomes were visualized by in-gel peptidase assay, using the fluorogenic peptide Suc-LLVY-AMC as a substrate. Two bands of 26S proteasome, corresponding to proteasome capped with one (RP_1CP) or two (RP_2CP) 19S RPs were easily discerned in wild-type extracts (Fig. 4*A*, *upper panel*), in agreement with what has been published in the past (23, 31).

The intensity of these 26S bands in samples obtained from *rpt2RF* extracts was dramatically diminished (Fig. 4*A*, *upper panel*), representing a significant proteolytic defect in these proteasomes, in agreement with what has been previously reported (31). To test whether the 26S is somewhat less stable in *rpt2RF* (hampering its proteolytic capacity) and to correctly assay for free 20S which in its latent form is undetected by the direct in-gel peptidase assay, we repeated the above experiment following preincubation of extracts with salt to dissociate 19S from 20S and activating the released 20S CP with minute amounts of SDS thus providing an estimate of the total 20S CP, whether "free" or naturally incorporated into 26S holoenzymes (Fig. 4*A*, *lower panel*). Significantly, upon 19S removal, the 20S released from *rpt2RF* displayed wild-type activity (Fig. 4*A*, *lower panel*). The Rpt2RF-containing proteasomes form stable 26S complexes that sustain electrophoresis and their 20S particles are proteolytically active, yet the *in vitro* proteolytic activity of the 26S particles is impaired (31). Hence, the impaired ERAD in *rpt2RF* reflects a general role played by Rpt2 in global proteasomal activity, most probably in controlling the opening of the 20S proteolytic chamber (28), which is likely to affect proteolysis of most (or all) proteasomal substrates, including ERAD substrates.

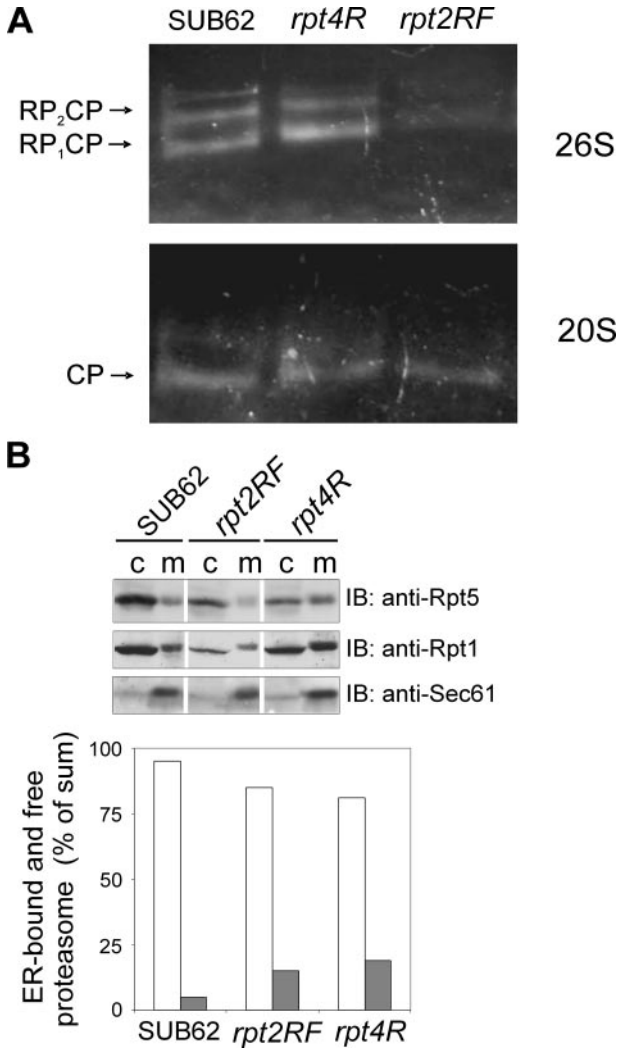

FIGURE 4. **Rpt4R-containing proteasome is structurally stable and proteolytically active and its ER association is not impaired.** *A*, post-nuclear supernatant (*PNS*) prepared by disrupting rapidly growing SUB62 (WT), *rpt2RF* and *rpt4R* strains was cleared by centrifugation (14,000 rpm, 10 min, 4 °C), and equal amounts of protein were loaded onto non-denaturing PAGE either as untreated 26S particles (*upper panel*) or as 20S particles dissociated from 19S (*lower panel*). The fluorogenic substrate Suc-LLVY-AMC was used for in-gel peptidase assay to visualize proteasome bands. *RP_2CP*, doubly capped proteasome; *RP_1CP*, singly capped proteasome; *20S*, free CP (below detection in rapidly growing cells, where 26S proteasomes predominate (15)). *B*, spheroplast from SUB62 (WT), *rpt2RF* or *rpt4R* strains were disrupted, microsomal pellets (*m*, 100% of sample) and cytosolic supernatants (*c*, 30% of sample) were separated from PNS by centrifugation (10,000 × *g*, 10 min, 4 °C), samples were dissolved, resolved by SDS-PAGE and immunoblotted (*IB*) with anti-Rpt1 (*middle panel*) and re-probed with anti-Rpt5 (*upper panel*) antibodies. Fractionation was assessed by re-probing with an anti-Sec61 antibody (*lower panel*). Blots were quantified by densitometry, and the diagram represents the equal distribution of Rpt1 or Rpt5 at the cytosolic face of the ER membrane (*gray bars*) or in the cytosol (*white bars*), as percent of total Rpts (sum of microsomes and cytosol).

The in-gel peptidase assay revealed that the Rpt4R-containing proteasomes were markedly different than the Rpt2RF-containing proteasomes. Clearly, the Rpt4R-containing proteasomes resembled the wild-type proteasomes, which both display similar assembly into 26S particles and show indistinguishable *in vitro* peptidase activity of their 26S and 20S particles (Fig. 4*A*). In contrast to the evident stabilization of two ERAD substrates in *rpt4R* (Fig. 1), Rpt4R-containing 26S pro-

teasomes are stable and exhibit normal *in vitro* peptidase activity (Fig. 4) and adequate *in vivo* proteolysis of cytosolic substrates (Fig. 2). These findings assign to the Rpt4 AAA-ATPase a preferential role in ERAD.

A preferential function in ERAD could be related to the ER-association of proteasomes, which is mediated by Rpt subunits (49). Hence, if Rpt4 plays a role in the proteasome ER-association, fractionation of proteasomes with the ER should be impaired in *rpt4R*. Fig. 4*B* shows the proteasomes distribution in the cytosol and in association with the Sec61-containing ER-derived microsomes. In fact, a larger fraction (~20%) of Rpt4R-containing proteasomes was ER-associated, compared with a small fraction (~5%) of wild-type proteasomes and a similar fraction (~15%) of Rpt2RF-containing proteasomes. Thus, it appears that the defective ERAD phenotype in *rpt4R* is neither the consequence of altered proteasome assembly or proteolytic activity, nor impaired ER-association. On the contrary, a slight enrichment of ER-associated proteasomes may be a consequence rather than the cause of ERAD deficiency in *rpt4R*.

Cell Fractionation and Protease Protection Assay Confirms the Involvement of Rpt4 in Dislocation of Luminal ERAD Substrates—To further understand the preferential involvement of Rpt4 in ERAD, we monitored localization and distribution of a luminal ERAD substrate following cell fractionation and protease protection assays (12). Significant differences in CPY*-HA distribution between wild-type, *rpt2RF*, and *rpt4R* were clearly observed (Fig. 5*A*). In wild-type, ~70% of CPY*-HA was microsomal, while only ~30% was cytosolic. However, the majority (~80%) of microsomal CPY*-HA was trypsin-sensitive and only ~20% was protected within the ER lumen (Fig. 5*B*). This distribution indicates that, under normal conditions, CPY*-HA tends to accumulate at the ER cytosolic face.

A slightly different picture was exhibited in *rpt2RF* cells. A larger CPY*-HA fraction (~50%) accumulated in cytosol, reflecting its impaired degradation by proteasomes with obstructed access to their proteolytic chamber. Of the remaining ~50% of microsomal CPY*-HA, ~70% was trypsin-sensitive and only ~30% was protected within the ER lumen (Fig. 5, *A* and *B*), resembling the wild-type ratio. The distribution of CPY*-HA in *rpt4R* cells was remarkably different, with ~60% microsomal and ~40% cytosolic. Importantly, about 80% of the microsomal CPY*-HA was protected from trypsin and only ~20% was trypsin-sensitive (Fig. 5, *A* and *B*), demonstrating that relative to wild-type or *rpt2RF*, a substantially larger fraction of the substrate accumulated within the ER lumen in *rpt4R* cells. To conclude, the cell fractionation and UPR experiments indicate that Rpt4 contributes primarily to the dislocation of ERAD substrates across ER membranes, whereas Rpt2 functions globally in proteasomal degradation.

Overexpression of Cdc48 Suppresses the ERAD Deficiency in rpt4R Mutant but Not the Impaired Proteasomal Degradation in rpt2RF or 20S Mutants—The above results indicate that Rpt4 is involved in dislocation of ERAD substrates, a role that has already been assigned to Cdc48, another AAA-ATPase (12). Using a similar approach, we have shown that Cdc48, an essential ERAD component, provides the driving force for passage of CPY*-HA across ER membranes (9, 12). Hence, CPY*-HA is

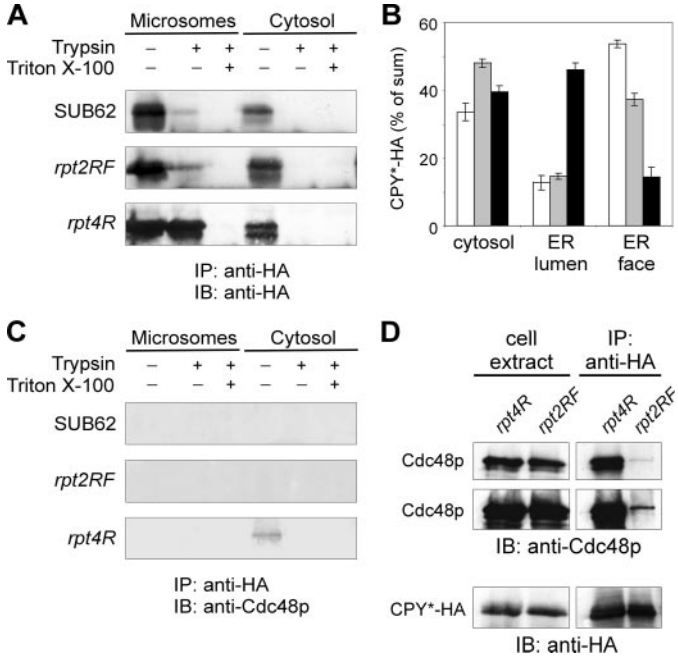

FIGURE 5. **Involvement of Rpt subunits in dislocation of CPY*-HA from the ER.** *A* and *C*, spheroplasts from wild-type (SUB62), *rpt2RF* or *rpt4R* strains expressing CPY*-HA were disrupted and PNS was treated with (+) or without (−) trypsin together (+) or without (−) Triton X-100. Microsomal pellets and cytosolic supernatants were separated by centrifugation, samples were dissolved, CPY*-HA was immunoprecipitated (*IP*) with an anti-HA antibody, resolved by SDS–PAGE, immunoblotted (*IB*) with an anti-HA antibody (*A*), and re-probed with an anti-Cdc48 antibody (*C*). *B*, diagram illustrates CPY*-HA distribution in ER lumen (microsomes treated with trypsin), at the ER cytosolic face (subtracting microsomes treated with trypsin from untreated microsomes) or in cytosol (untreated cytosol), as percent of total CPY*-HA (sum of untreated microsomes and untreated cytosol) in wild-type (*white bars*), *rpt2RF* (*gray bars*), or *rpt4R* (*black bars*). Distribution was quantified by densitometry and calculated as average (±S.E.) of five independent experiments represented by blots in *A*. *D*, *rpt2RF* and *rpt4R* strains expressing CPY*-HA were dissolved and CPY*-HA was immunoprecipitated with an anti-HA antibody. Cell extract (5% of sample) and immunoprecipitated (IP) CPY*-HA were resolved by SDS-PAGE and immunoblotted (*IB*) with an anti-Cdc48 antibody (*upper* and *middle panels*; short and long exposures, respectively) and re-probed with an anti-HA antibody (*lower panel*).

similarly trapped within the ER lumen in either *cdc48-10* at 37 °C (12) or in *rpt4R* (Fig. 5). To comprehend the intriguing functional interrelations between these two AAA-ATPases, we looked at the effect of Rpt4 activity on Cdc48 interaction with ERAD substrates. Immunoprecipitated CPY*-HA pulled down appreciable amounts of Cdc48 from *rpt4R* extracts, but hardly any from *rpt2RF* extracts, although both ERAD-defective strains accumulated CPY*-HA to the same level and contained abundant Cdc48 (Fig. 5*D*). Moreover, upon fractionation, the accumulating CPY*-HA pulled down Cdc48 from cytosolic fractions of *rpt4R*, but neither from *rpt4R* microsomal fractions, nor from any fractions of wild-type or *rpt2RF* (Fig. 5*C*). It suggests that Rpt4 activity is required for dissociation of ERAD substrates from Cdc48.

Although not suggested by sequence comparison or domain organization, Cdc48/p97 is functionally similar to proteasomal Rpt subunits (50), both belonging to the AAA-ATPases family. To further understand the functional interrelations between Cdc48 and Rpt4, excess Cdc48 was expressed from a plasmid in *rpt2RF* and *rpt4R* and its impact on CPY*-HA degradation was followed. Interestingly, ERAD deficiency in *rpt4R* was partly

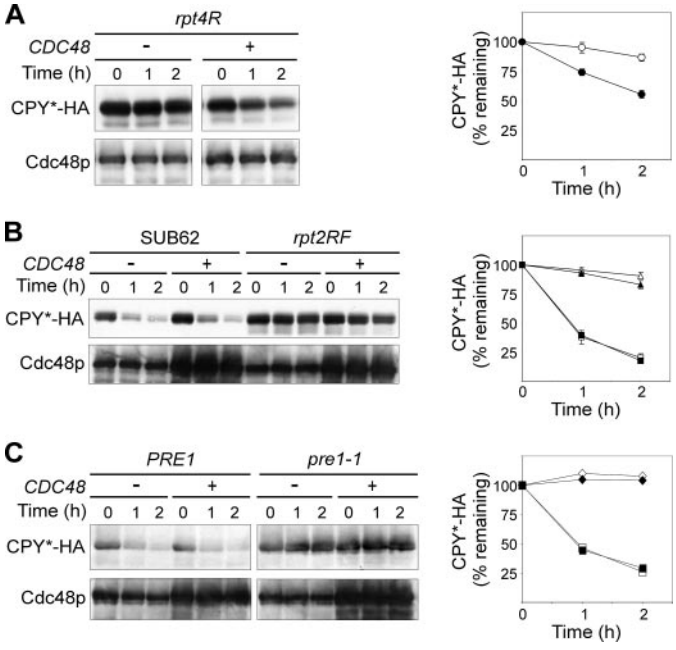

FIGURE 6. **Overexpression of Cdc48 suppresses ERAD deficiency in *rpt4R* but neither in *rpt2RF* nor in *pre1-1* mutants.** CPY*-HA-expressing plasmid was introduced together with (+; closed symbols) or without (−; open symbols) a Cdc48-expressing plasmid into *rpt4R* (*A*) *rpt2RF* (*B*) or *pre1–1* (*C*), and to their corresponding wild-type strains SUB62 (*B*) or *PRE1* (*C*). CPY*-HA degradation was followed by cycloheximide chase. Cells (2 A_{600}) were collected at the indicated time points, lysed, total cellular proteins were resolved by SDS-PAGE, and immunoblotted (*IB*) with an anti-HA antibody (*upper panels*) and re-probed with an anti-Cdc48 antibody (*lower panels*). Graphs illustrate degradation as amounts of remaining substrate as % of its level upon cycloheximide addition (100%), estimated by densitometry and calculated as average (±S.E.) of 5–7 independent experiments represented by the presented blots. Half-life values were calculated from the slopes of exponential curves (see text). Wild-type (SUB62, *PRE1*), *squares*; *rpt2RF*, *triangles*; *rpt4R*, *circles*; *pre1–1*; *diamonds*.

restored by excess Cdc48, shortening CPY*-HA half-life from >7 to ~2 h (Fig. 6*A*), which was only about 2-fold slower than the $t_{½}$ in wild-type. Conversely, excess Cdc48 was unable to rescue the defective CPY*-HA turnover in mutants exhibiting general proteasomal defects, such as *rpt2RF* ($t_{½}$ remained >7 h irrespective of Cdc48 expression; Fig. 6*B*), or *pre1-1* (Fig. 6*C*). Taken together, these results demonstrate that excess Cdc48 specifically suppresses ERAD deficiency in *rpt4R*, but cannot restore globally impaired proteasomal functions. We propose that both Cdc48 and Rpt4 contribute to the passage of CPY*-HA across ER membranes, while Rpt2 plays an essential downstream role in proteasomal degradation.

DISCUSSION

Evidently, ERAD does not represent a unique degradation pathway, because it eventually converges onto the ubiquitin system, where the proteasome acts as the end-point executing protease. However, several lines of evidence implicate the proteasome in earlier steps of ERAD upstream to its final role in proteolysis. Pinpointing the unique participation of the proteasome in ERAD has remained an important unresolved question in attempts to decipher this multistep ER-associated pathway. Here we address this point directly and systematically by comparing proteasomal degradation of ERAD and cytosolic substrates in proteasomal mutants harboring equivalent substitutions in the Walker A ATP-binding motifs in each of the Rpt ATPase subunits. Interestingly, equivalent *rpt* mutants display distinct phenotypes suggesting a measure of no redundancy. Specifically, we have uncovered a role for Rpt4 in a proximal ERAD-specific event, whereas Rpt2 functions at a distal step common to all proteasomal processes.

The proteasomal Rpt subunits are essential proteins that form a hetero-hexameric AAA-ATPase at the base of the 19S RP. Structural and functional homology of the Rpt subunits to other ATPase regulators of analogous proteases such as archaeal PAN (51) or bacterial ClpX (52) suggests that ATP hydrolysis is required for protein degradation by the 26S proteasome because the eukaryotic 19S RP unfolds and actively translocates substrates into the 20S catalytic chamber (25). However, as shown here for ERAD and as previously reported for other proteasomal reactions (31), the various 19S Rpt subunits are not functionally equivalent. We show that out of the six Rpt subunits, only Rpt2 and Rpt4 are pertinent to ERAD, although the contribution of Rpt4 is distinct from that of Rpt2. Rpt2 appears to act as an essential and common factor that operates at a later stage and contributes globally to the proteasomal proteolytic activity. This property of Rpt2 can be explained by its role in opening the 20S proteolytic chamber (28). By controlling the rate-limiting step of substrate access into the proteolytic chamber and subsequent hydrolysis, Rpt2 activity limits the flux through the proteasome and as such should influence any proteasomal proteolysis. This was shown *in vitro* for cleavage of short peptides, and *in vivo* in degradation of various proteasomal substrates, including the UFD substrate Ub-Pro-βgal, the "N-end rule" substrate Lys-βgal, the HO nuclear protein, the yeast-expressed mammalian NFκB and the transcription factor Ime1 (31, 45–47), and is now shown here for cytosolic ΔssCPY*-GFP and small peptides (Figs. 2 and 4). All these substrates are stabilized in *rpt2RF*. That the access to the 20S catalytic chamber is rate-limiting also in ERAD is demonstrated here for the *in vivo* degradation of luminal (CPY*-HA) and membrane (6myc-Hmg2) ERAD substrates. This conclusion is further supported by our recent finding that deletion of α3 and α7 N termini accelerates the *in vivo* degradation of the same repertoire of ERAD substrates (16).

Contrary to Rpt2, an equivalent mutation in Rpt4 does not affect downstream events of general proteasomal degradation. Neither cleavage of a short fluorogenic peptide *in vitro* nor degradation of a cytosolic substrate *in vivo* is hampered in *rpt4R*, yet ERAD of membrane 6myc-Hmg2 and luminal CPY*-HA is severely impaired. Thus, the non-redundant functions of Rpt4 are primarily in the ERAD pathway. Specifically, we find that Rpt4 activity is required for passage of substrates across ER membranes in the ERAD-specific dislocation step. Of all the equivalent *rpt* mutants that we tested, the most severe impairment of ERAD was in *rpt4R*, leading to a marked decrease in degradation of both luminal and membrane ERAD substrates. The resistance of *rpt4R* cells to tunicamycin as well as the activation and remarkable induction of UPR in the *rpt4R* mutant all support a direct and non overlapping role of Rpt4 in ERAD. Stabilization of CPY* in *rpt4R* was previously reported, but this protein was still dislocated in *rpt4R* (10). Here we show that in *rpt4R* the stabilized CPY*-HA accumulates within the lumen of

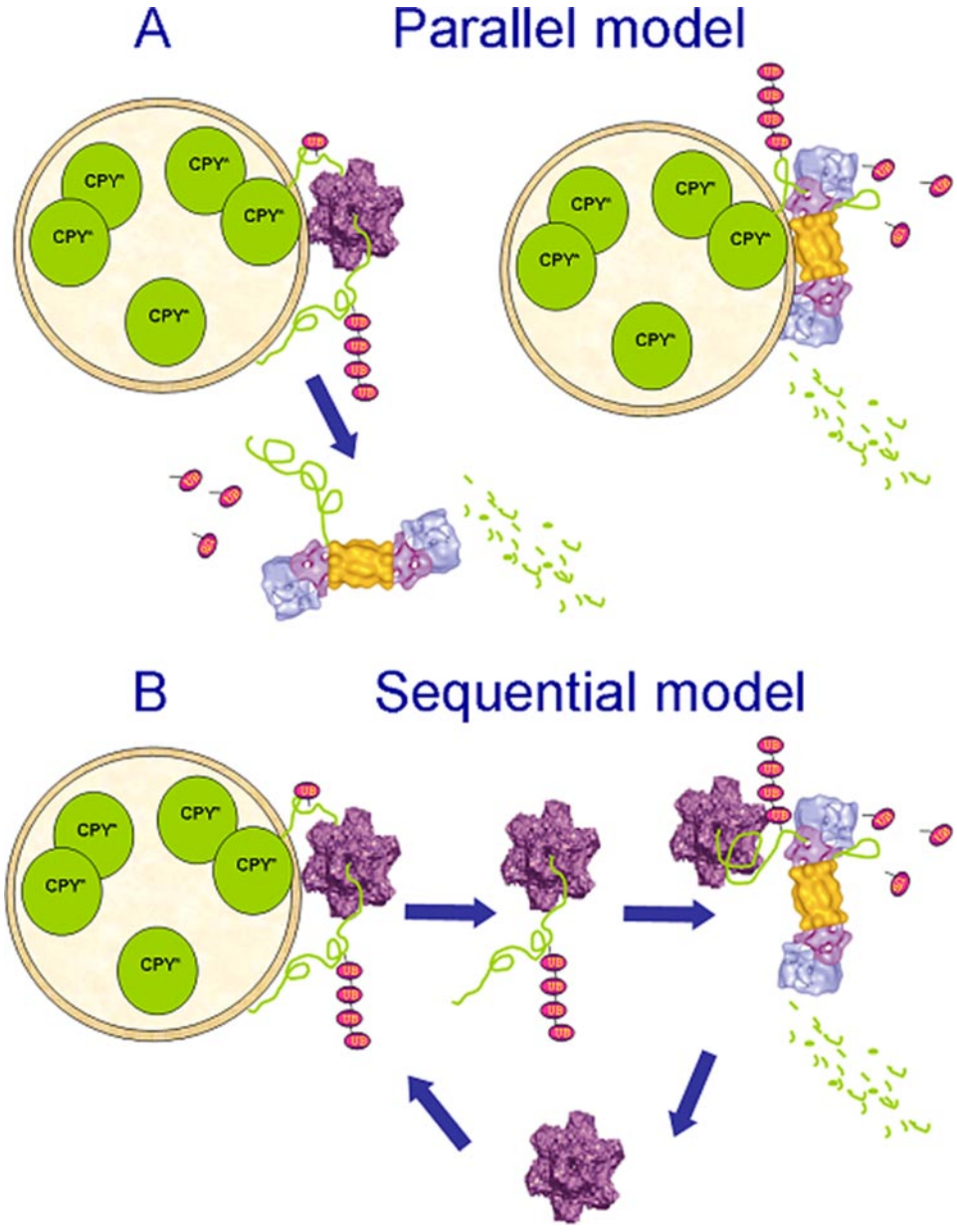

FIGURE 7. **Models of Rpt4 and Cdcd48 cooperation in ERAD.** *A*, parallel model. *B*, sequential model. Note that Rpt4 is part of the proteasome, and the proteasome itself, along with its Rpt subunits, is common to both models.

microsomes, in stark contrast to the situation in wild-type or *rpt2RF* strains (Fig. 5). Participating in passage of ERAD substrates across ER membranes explains how Rpt4 affects ER stress, UPR, and ERAD. Accumulation of unfolded ERAD substrates in the ER activates UPR and endows the *rpt4R* cells with a phenomenal capacity to cope with ER stress.

The alternate use of *rpt2* and *rpt4* mutants and the comparison of a luminal ERAD substrate alongside its cytosolic counterpart allow us to disentangle a very complex multistep pathway such as ERAD. We shed light on prominent rate-limiting steps and assign unique roles to Rpt2 and Rpt4. After passage across ER membranes, dislocated substrates are either proteolysed by ER-bound proteasome (12) or released to cytosol for proteolysis by free proteasomes. Hence, accumulation of luminal CPY* at ER cytosolic face (Fig. 5; and also (6)) points to either of these options as being rate-limiting in wild-type. Inactivation of Rpt2 yields inhibited "closed" proteasomes, and thus proteolysis gains prominence as the only rate-limiting step. Such "closed" proteasomes in *rpt2RF* similarly lead to stabilization of cytosolic ΔssCPY*-GFP and explains why luminal CPY*-HA accumulates in cytosol. It remains to be determined whether proteolysis of CPY*-HA is carried out by free proteasomes or this substrate is released and accumulates in cytosol only if the ER-bound proteasomes are clogged and incapacitated. Importantly, passage across ER membrane proceeds unaffected in *rpt2RF*, with the bottle-neck shifting to the terminal proteolysis. Inactivation of Rpt4 results in a proteolytically-active proteasome, as evidenced in the current study by the robust degradation of a cytosolic substrate and of small peptides. Yet, ERAD substrates are stabilized and CPY*-HA remains largely entrapped within the ER lumen, pinpointing the passage across ER membranes as the impaired ERAD step in *rpt4R*.

The involvement of Rpt4 in the passage of luminal CPY*-HA across ER membranes is surprising, given that this function is largely ascribed to p97/Cdc48 (8, 12). However, both Cdc48 and Rpt subunits are hexameric AAA-ATPases that share striking functional similarities (50) and both complexes are able to bind ubiquitin conjugates (29, 53). So it is plausible that Cdc48 and Rpt subunits collaborate with, or even replace, each other in their various roles in ERAD. This intriguing possibility is supported by our finding that impaired ERAD in *rpt4R* is partially restored by excess Cdc48 (Fig. 6). The inability of excess Cdc48 to restore ERAD when Rpt2 is dysfunctional suggests that homo-hexameric Cdc48 does not replace the hetero-hexameric Rpt at the base of the proteasomal 19S RP but rather cooperates with the proteasome.

Two possible models may explain Cdc48 and Rpt4 cooperation in the ERAD-specific dislocation process. In a parallel model (Fig. 7*A*), both AAA-ATPases pull substrates across ER membranes. In a sequential model (Fig. 7*B*), Cdc48 pulls ERAD substrates across ER membranes while Rpt4 is required for delivering substrates from Cdc48 to 26S proteasomes. The parallel model is supported by the 19S RP being the sole driving force for the *in vitro* dislocation of pro-alpha factor (21). More-

over, although proteasomes are largely free in the cytosol, its ER association should facilitate its function in pulling substrates out of the ER and indeed, only a small subpopulation of ER-bound proteasomes interacts with the luminal ERAD substrate μs (12). Interestingly, the salt-sensitive, ATP-dependent association of proteasomes with ER membranes is mediated by high affinity binding of the Rpt-containing base of the 19S RP (49).

In the sequential model, pulling ERAD substrates out of the ER is facilitated by Cdc48, which, in turn, delivers substrates to proteasomes that are either ER-bound or free in the cytosol. In our model we depicted the option of free proteasome (Fig. 7*B*) because Cdc48 that remained associated with CPY*-HA in *rpt4R* was detected in the cytosol (Fig. 5*C*). The sequential model renders the proteasome ER-binding irrelevant to its role in ERAD, whereas Cdc48 ER-binding is crucial. It appears that p97/Cdc48 that operates in ERAD is indeed ER-bound. Although p97 is mostly free in the cytosol, μs pulls down only the small subpopulation of the ER-bound p97 (12). Binding of p97 to ER membranes is mediated by VIMP and Derlin-1 (54), and p97 interacts directly with several ER-localized ubiquitin ligases (55–57). In yeast, Ubx2/Sel1 is required for ERAD because it recruits Cdc48 to the ER, and mediates binding of Cdc48 to ERAD-dedicated ER-localized ubiquitin ligases, to ERAD substrates and to Der1 and Dfm1 (58, 59). Thus, one may envisage a scenario in which Cdc48 and Rpt4 function sequentially such that ER-bound Cdc48 pulls ERAD substrate across ER membranes and delivers them to proteasomes. The Rpt4 activity is required to accept substrates and release Cdc48 for an additional pulling cycle. This scenario concurs with the role of ATP hydrolysis in modulating 26S proteasome associations (24) and with our finding that in *rpt4R*, Cdc48 maintains prolonged association with ERAD substrates.

Our finding that excess Cdc48 partially restores impaired ERAD when Rpt4 is rendered dysfunctional is compatible with both models: in the parallel model, excess Cdc48 can compensate for the absence of Rpt4 as the puller; in the sequential model, excess Cdc48 can compensate for the absence of active free Cdc48 that remains occupied with the undelivered substrate.

Acknowledgments—We thank Efrat Grinboim for valuable contribution and the members of our groups and Dr. Joseph Roitelman for critical reading of the manuscript.

REFERENCES

1. Schubert, U., Anton, L. C., Gibbs, J., Norbury, C. C., Yewdell, J. W., and Bennink, J. R. (2000) *Nature* **404,** 770–774
2. Glickman, M. H., and Ciechanover, A. (2002) *Physiol. Rev.* **82,** 373–428
3. Bonifacino, J. S., and Weissman, A. M. (1998) *Annu. Rev. Cell Dev. Biol.* **14,** 19–57
4. Lederkremer, G. Z., and Glickman, M. H. (2005) *Trends Biochem. Sci.* **30,** 297–303
5. Bar-Nun, S. (2005) *Curr. Top. Microbiol. Immunol.* **300,** 95–125
6. Hiller, M. M., Finger, A., Schweiger, M., and Wolf, D. H. (1996) *Science* **273,** 1725–1728
7. Bays, N. W., Wilhovsky, S. K., Goradia, A., Hodgkiss-Harlow, K., and Hampton, R. Y. (2001) *Mol. Biol. Cell* **12,** 4114–4128
8. Ye, Y., Meyer, H. H., and Rapoport, T. A. (2001) *Nature* **414,** 652–656
9. Rabinovich, E., Kerem, A., Frohlich, K. U., Diamant, N., and Bar-Nun, S. (2002) *Mol. Cell Biol.* **22,** 626–634
10. Jarosch, E., Taxis, C., Volkwein, C., Bordallo, J., Finley, D., Wolf, D. H., and Sommer, T. (2002) *Nat. Cell Biol.* **4,** 134–139
11. Ye, Y., Meyer, H. H., and Rapoport, T. A. (2003) *J. Cell Biol.* **162,** 71–84
12. Elkabetz, Y., Shapira, I., Rabinovich, E., and Bar-Nun, S. (2004) *J. Biol. Chem.* **279,** 3980–3989
13. Rouiller, I., DeLaBarre, B., May, A. P., Weis, W. I., Brunger, A. T., Milligan, R. A., and Wilson-Kubalek, E. M. (2002) *Nat. Struct. Biol.* **9,** 950–957
14. Lupas, A. N., and Martin, J. (2002) *Curr. Opin. Struct. Biol.* **12,** 746–753
15. Bajorek, M., Finley, D., and Glickman, M. H. (2003) *Curr. Biol.* **13,** 1140–1144
16. Rabinovich, E., Bajorek, M., Glickman, M., and Bar-Nun, S. (2006) *Israel J. Chem.* **46,** 219–224
17. Rivett, A. J. (1998) *Curr. Opin. Immunol.* **10,** 110–114
18. Hirsch, C., and Ploegh, H. L. (2000) *Trends Cell Biol.* **10,** 268–272
19. Mayer, T. U., Braun, T., and Jentsch, S. (1998) *EMBO J.* **17,** 3251–3257
20. Elkabetz, Y., Kerem, A., Tencer, L., Winitz, D., Kopito, R. R., and Bar-Nun, S. (2003) *J. Biol. Chem.* **278,** 18922–18929
21. Lee, R. J., Liu, C. W., Harty, C., McCracken, A. A., Latterich, M., Romisch, K., DeMartino, G. N., Thomas, P. J., and Brodsky, J. L. (2004) *EMBO J.* **23,** 2206–2215
22. DeMartino, G. N., Moomaw, C. R., Zagnitko, O. P., Proske, R. J., Chuping, M., Afendis, S. J., Swaffield, J. C., and Slaughter, C. A. (1994) *J. Biol. Chem.* **269,** 20878–20884
23. Glickman, M. H., Rubin, D. M., Fried, V. A., and Finley, D. (1998) *Mol. Cell Biol.* **18,** 3149–3162
24. Verma, R., Chen, S., Feldman, R., Schieltz, D., Yates, J., Dohmen, J., and Deshaies, R. J. (2000) *Mol. Biol. Cell* **11,** 3425–3439
25. Braun, B. C., Glickman, M., Kraft, R., Dahlmann, B., Kloetzel, P. M., Finley, D., and Schmidt, M. (1999) *Nat. Cell Biology* **1,** 221–226
26. Groll, M., Bajorek, M., Kohler, A., Moroder, L., Rubin, D. M., Huber, R., Glickman, M. H., and Finley, D. (2000) *Nat. Struct. Biol.* **7,** 1062–1067
27. Kohler, A., Bajorek, M., Groll, M., Moroder, L., Rubin, D. M., Huber, R., Glickman, M. H., and Finley, D. (2001) *Biochimie (Paris)* **83,** 325–332
28. Kohler, A., Cascio, P., Leggett, D. S., Woo, K. M., Goldberg, A. L., and Finley, D. (2001) *Mol. Cell* **7,** 1143–1152
29. Lam, Y. A., Lawson, T. G., Velayutham, M., Zweier, J. L., and Pickart, C. M. (2002) *Nature* **416,** 763–767
30. Hill, K., and Cooper, A. A. (2000) *EMBO J.* **19,** 550–561
31. Rubin, D. M., Glickman, M. H., Larsen, C. N., Dhruvakumar, S., and Finley, D. (1998) *EMBO J.* **17,** 4909–4919
32. Sung, P., Higgins, D., Prakash, L., and Prakash, S. (1988) *EMBO J.* **7,** 3263–3269
33. Heinemeyer, W., Kleinschmidt, J. A., Saidowsky, J., Escher, C., and Wolf, D. H. (1991) *EMBO J.* **10,** 555–562
34. Medicherla, B., Kostova, Z., Schaefer, A., and Wolf, D. H. (2004) *EMBO Rep.* **5,** 692–697
35. Fu, H., Reis, N., Lee, Y., Glickman, M. H., and Vierstra, R. D. (2001) *EMBO J.* **20,** 7096–7107
36. Jungmann, J., Reins, H. A., Schobert, C., and Jentsch, S. (1993) *Nature* **361,** 369–371
37. Wang, Q., and Chang, A. (2003) *EMBO J.* **22,** 3792–3802
38. Elbein, A. D. (1987) *Annu. Rev. Biochem.* **56,** 497–534
39. Zhou, M., and Schekman, R. (1999) *Mol. Cell* **4,** 925–934
40. Kawahara, T., Yanagi, H., Yura, T., and Mori, K. (1997) *Mol. Biol. Cell* **8,** 1845–1862
41. Leggett, D. S., Glickman, M. H., and Finley, D. (2005) *Methods Mol. Biol.* **301,** 57–70
42. Smith, D. M., Kafri, G., Cheng, Y., Ng, D., Walz, T., and Goldberg, A. L. (2005) *Mol. Cell* **20,** 687–698
43. Benaroudj, N., Zwickl, P., Seemuller, E., Baumeister, W., and Goldberg, A. L. (2003) *Mol. Cell* **11,** 69–78
44. Hampton, R. Y., Gardner, R. G., and Rine, J. (1996) *Mol. Biol. Cell* **7,** 2029–2044
45. Sears, C., Olesen, J., Rubin, D., Finley, D., and Maniatis, T. (1998) *J. Biol. Chem.* **273,** 1409–1419
46. Guttmann-Raviv, N., Martin, S., and Kassir, Y. (2002) *Mol. Cell Biol.* **22,** 2047–2056
47. Kaplun, L., Ivantsiv, Y., Kornitzer, D., and Raveh, D. (2000) *Proc. Natl. Acad. Sci. U. S. A.* **97,** 10077–10082

48. Urano, F., Calfon, M., Yoneda, T., Yun, C., Kiraly, M., Clark, S. G., and Ron, D. (2002) *J. Cell Biol.* **158,** 639–646
49. Kalies, K. U., Allan, S., Sergeyenko, T., Kroger, H., and Romisch, K. (2005) *EMBO J.* **24,** 2284–2293
50. Elsasser, S., and Finley, D. (2005) *Nat. Cell Biol.* **7,** 742–749
51. Navon, A., and Goldberg, A. L. (2001) *Mol. Cell* **8,** 1339–1349
52. Ortega, J., Singh, S. K., Ishikawa, T., Maurizi, M. R., and Steven, A. C. (2000) *Mol. Cell* **6,** 1515–1521
53. Dai, R. M., and Li, C. C. (2001) *Nat. Cell Biol.* **3,** 740–744
54. Ye, Y., Shibata, Y., Yun, C., Ron, D., and Rapoport, T. A. (2004) *Nature* **429,** 841–847
55. Zhong, X., Shen, Y., Ballar, P., Apostolou, A., Agami, R., and Fang, S. (2004) *J. Biol. Chem.* **279,** 45676–45684
56. Ye, Y., Shibata, Y., Kikkert, M., van Voorden, S., Wiertz, E., and Rapoport, T. A. (2005) *Proc. Natl. Acad. Sci. U. S. A.* **102,** 14132–14138
57. Lilley, B. N., and Ploegh, H. L. (2005) *Proc. Natl. Acad. Sci. U. S. A.* **102,** 14296–14301
58. Schuberth, C., and Buchberger, A. (2005) *Nat. Cell Biol.* **7,** 999–1006
59. Neuber, O., Jarosch, E., Volkwein, C., Walter, J., and Sommer, T. (2005) *Nat. Cell Biol.* **7,** 993–998
60. Rabinovich, E., D. Bussi, I. Shapira, G. Alalouf, C. Lipson, Y. Elkabetz, M. Glickman, M. Bajorek, and S. Bar-Nun. (2006) *Isr. Med. Assoc. J.* **8,** 238–242

A Proteasomal ATPase Contributes to Dislocation of Endoplasmic Reticulum-associated Degradation (ERAD) Substrates

Carni Lipson, Guy Alalouf, Monika Bajorek, Efrat Rabinovich, Avigail Atir-Lande, Michael Glickman and Shoshana Bar-Nun

J. Biol. Chem. 2008, 283:7166-7175.
doi: 10.1074/jbc.M705893200 originally published online January 3, 2008
